Monitoring and quantitative evaluation of Faraday cup deterioration in a thermal ionization mass spectrometer using multidynamic analyses of laboratory standards

Yankun Di*[a], Zefeng Li[b], Yuri Amelin[a]

[a] Research School of Earth Sciences, Australian National University, Acton, ACT 2601, Australia

[b] Research School of Astronomy & Astrophysics, Australian National University, Weston Creek, ACT 2611, Australia

*Corresponding author, email: yankun.di@anu.edu.au

Submitted to *Journal of Analytical Atomic Spectrometry* as a full paper

Significance to JAAS

This paper presents a new method for characterization of the changes in performance of arrays of detectors, e.g., Faraday cups, in isotope ratio mass spectrometry. The method provides a simple way to quantitatively and continuously track the change of detector efficiency, an important factor that controls the accuracy and precision of isotope analyses. The advantage of this method compared to the existing methods is that it can be fast and easily performed within the laboratory's routine isotope analyses without the need of additional, specially designed experiments. This method is applicable to all types of detectors and multi-collection mass spectrometers.

Abstract

Accurate and precise isotopic ratio determinations using multi-collector (MC) mass spectrometers rely on accurate cross-calibration and long-term stability of the efficiencies of the multiple detectors. Isotopic analyses at part per million (ppm) level of precision, which are commonly carried out with thermal ionization mass spectrometers (TIMS) equipped with arrays of several Faraday cups, are the most sensitive to detector efficiency variations. Quantitative characterization of Faraday cup efficiency changes (also known as Faraday cup deterioration) during instrument usage can assist the analyst in making decision about replacement or cleaning of Faraday cups, and in making corrections to measured isotopic ratios, which are both essential to sustain the high measurement accuracy and long-term reproducibility of MC–TIMS. In this study, we present a method to quantitatively and continuously track the deterioration degrees of individual Faraday cups on MC–TIMS. The advantage of this method, compared to previous ones, is that it uses only the results of regular repetitive analyses of laboratory standards, and no additional, specially designed experiments are required. Using this method, we monitored the performance of the Triton *Plus* MC–TIMS

at Research School of Earth Sciences, the Australian National University, during a 6-month Sr isotope analytical session, and observed significant Faraday cup deterioration up to 150 ppm. The cups that have received the most abundant Sr atom deposition during the analytical session deteriorated the most, confirming that the accumulation of measured elements is the likely cause of changing Faraday cup efficiencies. The response of cup efficiency to the accumulation of Sr atoms in the cup is complex and non-linear, and differs between cups in magnitude and direction, suggesting that Faraday cup deterioration is not a simple univariate function of the accumulation of measured elements.

1. Introduction

Isotopic ratio determination using mass spectrometers, including thermal ionization mass spectrometer (TIMS),[1, 2] inductively coupled plasma mass spectrometer (ICPMS),[3-7] and secondary ionization mass spectrometer (SIMS),[8] has seen a great precision improvement in the recent three decades owing to the application of the multi-collection (MC) technique.[9] Equipped with an array of multiple detectors (most commonly Faraday cups connected to electrometer amplifiers) in the detector chamber, MC mass spectrometers can simultaneously collect and detect ion beams with different mass/charge ratios separated by the analyser. Compared to the single collector mass spectrometers which employ a peak-jumping scan mode during isotopic ratio measurements, MC mass spectrometers operated in the static mode have three major advantages. First, the simultaneous measurements of multiple ion beam intensities completely remove the inaccuracy originated from signal instabilities related to the ion source. Correction for the signals' temporal drifting is therefore not needed, while the rapid and accidental fluctuations of signals do not influence the measured isotopic ratios. Second, simultaneous integration of multiple isotopes substantially reduces the duration of isotope

analyses compared to sequentially scanning all relevant masses. It also saves the time needed to change the magnetic field and to settle down the residual signals in amplifiers between integration steps, which are both essential in the peak-jumping mode. Third, the static measurement enables the ionized samples to be used more efficiently by detecting all generated ions, which allows analysis of smaller samples with the same targeted precision, or increasing precision for a given sample size due to better counting statistics. These virtues eventually enable isotopic ratios to be analysed with exceptionally high precision using MC mass spectrometers.[10-21]

Multi-collection mass spectrometers, however, have problems associated with variations of detector efficiencies that are inconsequential for single collector peak-jumping measurements. Two main components of detector efficiency in the commonly used ion beam registration channels made of Faraday cups connected to electrometer amplifiers are Faraday cup efficiency (FCE) and amplifier gain. Faraday cup efficiency is the ratio of the current flowing through the high-ohmage feedback resistor connected to the Faraday cup to the ion current injected into the Faraday cup. Amplifier gain is the conversion factor from the input electric current signal from the Faraday cup to the output voltage signal of the voltmeter. In multicollector systems used in isotopic ratio measurement, the efficiencies of the multiple detectors can slightly differ, and can independently vary over time. Amplifier gain varies depending on the accurate resistance of the high-ohmage feedback resistor, which in turn depends on the temperature in the amplifier housing and the current passing through the resistor. The value of FCE deviates from unity due to a series of complex factors, including the material, geometry, and surface properties of the cup, the incept angle, momentum, and intensity of the incoming ion beams, as well as the already analysed elements deposited on the surfaces of the cup.[1, 9, 10, 22, 23] As such, accurate isotopic ratio measurements using MC mass spectrometers require accurate knowledge and cross-calibration of detector efficiencies. The ultimate long-

term measurement precision using MC mass spectrometers depends on the stability of detector efficiencies.[24, 25]

Among all types of MC mass spectrometers, MC–TIMS is the most sensitive to such detector efficiency issue because of its high measurement precision and relatively low analytical dependence on reference standards.[23, 25, 26] During MC–TIMS analyses, amplifier gains can be measured and cross-calibrated by connecting the inputs of the amplifiers sequentially to a stable reference current and measuring the responses of the amplifiers. The uncertainty of amplifier gain calibration in mass spectrometers manufactured by Thermo Scientific can be further reduced by using the virtual amplifier utility[9] that switches connections between Faraday cups and amplifiers. However, eliminating the effect of FCE, the other component of detector efficiency, is not easy.

In principle, FCEs can be determined, and corrected for, using a procedure similar to amplifier gain calibration.[1, 27-30] This approach would require a source of constant and exceptionally stable ion beam that could be directed sequentially into all Faraday cups. Such source, however, is physically difficult to produce. The complete cancellation of FCEs during MC–TIMS analyses can also be achieved by standard–sample comparison, given that FCEs can be regarded constant between analyses. However, the temporal drift of FCEs along with instrument usage, also known as Faraday cup deterioration, in time scales from weeks to years have been reported.[1, 10-12, 25, 31-37] Reference standards thus have to be analysed more frequently to accurately capture the rapid changes of FCEs, resulting in reduced analytical efficiency and sample throughput of MC–TIMS. An alternative way to cancelling FCEs is to use a dynamic multi-collection (or "multidynamic") method in isotopic ratio measurements.[1, 10, 31] With cup positions fixed but the magnetic field settings dynamically switched within a measurement cycle, the isotopic ratio of interest and the isotopic ratio used to monitor mass fractionation can be sequentially measured using the same combination of Faraday cups, and hence FCEs can be

mathematically cancelled during fractionation correction.[10] However, even the isotopic ratios measured using multidynamic methods have been shown to be affected by Faraday cup deterioration.[10, 22, 25] With ongoing instrument usage, not only isotopic ratios drift due to the changes of FCEs, but also measurement precision deteriorates,[10, 32, 35] presumably due to the uneven distribution of deposition in the cups and the increasing sensitivity of secondary charged particle yield to the exact point of ion incidence.[1, 23] Multidynamic methods can effectively minimize the systematic errors (inaccuracy effect) caused by cup deterioration and improve the long-term measurement precision, but the enhanced random errors (imprecision effect) caused by cup deterioration is difficult to eliminate,[1, 10] unless the Faraday cups are replaced or mechanically cleaned.

Quantitative characterization of Faraday cup deterioration during isotopic analyses can assist the analyst in making decision about replacement or cleaning of Faraday cups, and in making corrections to measured isotopic ratios. Continuous monitoring the long-term drift trends of FCEs can also help us to better understand the physical mechanism behind cup deterioration. The systematic drifts of repetitively measured static isotopic ratios of reference standards have been documented in many studies and been proposed as an indicator of Faraday cup deterioration.[1, 10, 32, 35, 37] However, as shown by Garçon et al.[10] and also in the section 2 of this paper, a fractionation-corrected static isotopic ratio measured by MC–TIMS generally involves three FCE components. It is difficult to precisely determine, from the temporal drifts of the static isotopic ratios, which cups are deteriorating, ,by what degrees they are deteriorating, and whether the efficiency of each cup is increasing or decreasing.[10, 37] In our MC–TIMS laboratory, over a 6-month Sr isotope analytical session, we observed clear temporal drifts of statically measured $^{84}Sr/^{86}Sr$ and $^{87}Sr/^{86}Sr$ ratios of the standard NIST SRM 987, indicating that the Faraday cups used have significantly deteriorated during the analytical session. The purpose of this study, therefore, is to explore a method to quantitatively evaluate the deterioration

143 degrees of the individual Faraday cups using the available isotopic data of the standard acquired
144 during the session. We demonstrate the simplicity and effectiveness of this method using our
145 Sr isotope study case, and investigate the evolutionary trends of FCEs during our analytical
146 session. We also discuss the potential applicability of this method to the analyses of other
147 isotope systems.
148
149 **2. Experimental**
150 Over a 6-month session from April to October 2019, high-precision Sr isotope ($^{87}Sr/^{86}Sr$
151 and $^{84}Sr/^{86}Sr$) analyses of a large number of natural samples (mainly terrestrial and extra-
152 terrestrial rocks) and reference materials were performed at the MC–TIMS lab of Research
153 School of Earth Sciences, the Australian National University, using the method described
154 below. The Sr isotope standard NIST SRM 987 were repetitively and regularly analysed in the
155 session for 43 times, and those analyses were almost evenly distributed over time and
156 interspersed with the analyses of rocks and minerals.
157 Purified and evaporated samples containing 0.5–1 μg Sr were mixed with TaF_5
158 activator[38] and were loaded onto single Re filaments. The mixture solutions were dried by
159 supplying slowly increasing current up to ca. 2.3 A. Strontium isotopes were analysed using a
160 Thermo Scientific Triton *Plus* multicollector thermal ionization mass spectrometer. A 3-line
161 multidynamic cup configuration used for the analyses is shown in Table 1. Before each
162 measurement, amplifier gains were calibrated during filament heating. Measurements started
163 immediately when small Sr signals appeared, and were initially operated with increasing
164 filament temperature until the ^{88}Sr ion beam reached a steady intensity of ca. 2×10^{-10} A. The
165 following measurement was operated with the default inter-block heating/cooling function of
166 Triton to maintain the ion beam intensity stable. The measurement was stopped when the
167 sample was completely exhausted. One measurement typically consisted of 50–70 blocks of

10 cycles (i.e., 500–700 cycles). For all measurements, the amplifier matrix was rotated, the baseline was measured for 30 s before each block, and the peak centre and lens focus tuning were automatically repeated before each 5 blocks. The isobaric interference of ^{87}Rb on ^{87}Sr was monitored using ^{85}Rb, and was subtracted on-line assuming ^{87}Rb/^{85}Rb = 0.386.

For each cycle, static ^{84}Sr/^{86}Sr and ^{87}Sr/^{86}Sr ratios from the 3 magnetic settings (lines) were calculated by correcting mass fractionation to ^{88}Sr/^{86}Sr = 8.375209 using the exponential law[31] following the equations:

$$(^{84}\mathrm{Sr}/^{86}\mathrm{Sr})_{\mathrm{c,static\ line}\ i} = (^{84}\mathrm{Sr}/^{86}\mathrm{Sr})_{\mathrm{m,line}\ i} \cdot [\frac{8.375209}{(^{88}\mathrm{Sr}/^{86}\mathrm{Sr})_{\mathrm{m,line}\ i}}]^{\beta_{84}} \quad (1a)$$

$$(^{87}\mathrm{Sr}/^{86}\mathrm{Sr})_{\mathrm{c,static\ line}\ i} = (^{87}\mathrm{Sr}/^{86}\mathrm{Sr})_{\mathrm{m,line}\ i} \cdot [\frac{8.375209}{(^{88}\mathrm{Sr}/^{86}\mathrm{Sr})_{\mathrm{m,line}\ i}}]^{\beta_{87}} \quad (1b)$$

where "c" and "m" denotes "corrected" and "measured" respectively; i = 1, 2, or 3; β_{84} = –1.02325 and β_{87} = 0.50359, which were calculated using the relative atomic masses of isotopes from the International Union of Pure and Applied Chemistry (IUPAC).[39] In the static isotopic ratio calculations above, three Faraday cup efficiency components are involved in each fractionation-corrected isotopic ratio. For example, considering that Faraday cup efficiency (C) is defined as the measured/true ion beam current ($I_{measured}/I_{true}$), equation (1a) for line 1 can be rewritten as:

$$(^{84}\mathrm{Sr}/^{86}\mathrm{Sr})_{\mathrm{c,static\ line\ 1}} = (\frac{\mathrm{I}_{^{84}\mathrm{Sr}}}{\mathrm{I}_{^{86}\mathrm{Sr}}})_{\mathrm{true,line\ 1}} \cdot (\frac{\mathrm{C_{L1}}}{\mathrm{C_{H1}}}) \cdot [\frac{8.375209}{(\frac{\mathrm{I}_{^{88}\mathrm{Sr}}}{\mathrm{I}_{^{86}\mathrm{Sr}}})_{\mathrm{true,line\ 1}} \cdot (\frac{\mathrm{C_{H3}}}{\mathrm{C_{H1}}})}]^{\beta_{84}}$$

$$= (\frac{\mathrm{I}_{^{84}\mathrm{Sr}}}{\mathrm{I}_{^{86}\mathrm{Sr}}})_{\mathrm{true,line\ 1}} \cdot [\frac{8.375209}{(\frac{\mathrm{I}_{^{88}\mathrm{Sr}}}{\mathrm{I}_{^{86}\mathrm{Sr}}})_{\mathrm{true,line\ 1}}}]^{\beta_{84}} \cdot \mathrm{C_{L1}} \cdot \mathrm{C_{H3}}^{-\beta_{84}} \cdot \mathrm{C_{H1}}^{-1+\beta_{84}}$$

$$= (^{84}\mathrm{Sr}/^{86}\mathrm{Sr})_{\mathrm{unbiased\ line\ 1}} \cdot \mathrm{C_{L1}} \cdot \mathrm{C_{H3}}^{-\beta_{84}} \cdot \mathrm{C_{H1}}^{-1+\beta_{84}} \quad (1c)$$

where the "unbiased" ^{84}Sr/^{86}Sr ratio refers to the fractionation-corrected static ^{84}Sr/^{86}Sr ratio when all Faraday cup efficiencies are unity. Since β_{84} = –1.02325, equation (1c) indicates that 100%, 102%, and –202% of the relative efficiency changes of cup L1, H3, and H1 can be

propagated into the calculated $^{84}Sr/^{86}Sr$ ratio respectively. The equations for other lines can be rewritten with Faraday cup efficiencies similarly. Because amplifier gains were calibrated before each measurement, and the "amplifier rotation" function of Triton was activated to average the gain differences between amplifiers, the differences in amplifier gain are considered negligible here.

The $^{84}Sr/^{86}Sr$ and $^{87}Sr/^{86}Sr$ ratios from each cycle were also calculated using the multidynamic (MD) method. The $^{84}Sr/^{86}Sr$ ratio measured at line 1 and the $^{88}Sr/^{86}Sr$ ratio measured at line 3, which were sequentially measured using Faraday cups H1 + L1, were used in the multidynamic $^{84}Sr/^{86}Sr$ calculation:

$$(^{84}\mathrm{Sr}/^{86}\mathrm{Sr})_{\mathrm{c,MD}} = (^{84}\mathrm{Sr}/^{86}\mathrm{Sr})_{\mathrm{m,line\ 1}} \cdot \left[\frac{8.375209}{(^{88}\mathrm{Sr}/^{86}\mathrm{Sr})_{\mathrm{m,line\ 3}}}\right]^{\beta_{84}} \quad (2a)$$

where $\beta_{84} = -1.02325$. Equation (2*a*) can be rewritten with Faraday cup efficiencies:

$$(^{84}\mathrm{Sr}/^{86}\mathrm{Sr})_{\mathrm{c,MD}} = \left(\frac{\mathrm{I}_{^{84}\mathrm{Sr}}}{\mathrm{I}_{^{86}\mathrm{Sr}}}\right)_{\mathrm{true,line\ 1}} \cdot \left(\frac{\mathrm{C_{L1}}}{\mathrm{C_{H1}}}\right) \cdot \left[\frac{8.375209}{\left(\frac{\mathrm{I}_{^{88}\mathrm{Sr}}}{\mathrm{I}_{^{86}\mathrm{Sr}}}\right)_{\mathrm{true,line\ 3}} \cdot \left(\frac{\mathrm{C_{H1}}}{\mathrm{C_{L1}}}\right)}\right]^{\beta_{84}}$$

$$= \left(\frac{\mathrm{I}_{^{84}\mathrm{Sr}}}{\mathrm{I}_{^{86}\mathrm{Sr}}}\right)_{\mathrm{true,line\ 1}} \cdot \left[\frac{8.375209}{\left(\frac{\mathrm{I}_{^{88}\mathrm{Sr}}}{\mathrm{I}_{^{86}\mathrm{Sr}}}\right)_{\mathrm{true,line\ 3}}}\right]^{\beta_{84}} \cdot \left(\frac{\mathrm{C_{L1}}}{\mathrm{C_{H1}}}\right)^{1+\beta_{84}} \quad (2b)$$

Since $1 + \beta_{84} = -0.02325$, only ca. 2.3% of the relative cup efficiency C_{L1}/C_{H1} is propagated into the multidynamic $^{84}Sr/^{86}Sr$ ratio, and the remaining 97.7% is mathematically cancelled. Two multidynamic $^{87}Sr/^{86}Sr$ ratios can be calculated in our 3-line method using combined lines 1 + 2 and lines 2 + 3. The first multidynamic ratio, $(^{87}Sr/^{86}Sr)_{c,MD-A}$, was calculated by taking the geometric mean of the measured $^{87}Sr/^{86}Sr$ ratios of line 1 and line 2, followed by mass fractionation correction using the measured $^{88}Sr/^{86}Sr$ ratio of line 2:

$$(^{87}\mathrm{Sr}/^{86}\mathrm{Sr})_{\mathrm{c,MD-A}} = \sqrt{(^{87}\mathrm{Sr}/^{86}\mathrm{Sr})_{\mathrm{m,line\ 1}} \cdot (^{87}\mathrm{Sr}/^{86}\mathrm{Sr})_{\mathrm{m,line\ 2}}}$$

$$\cdot \left[\frac{8.375209}{(^{88}\mathrm{Sr}/^{86}\mathrm{Sr})_{\mathrm{m,line\ 2}}}\right]^{\beta_{87}} \quad (3a)$$

where β_{87} = 0.50359. Considering Faraday cup efficiencies, equation (3*a*) can be rewritten as:

$$(^{87}Sr/^{86}Sr)_{c,MD-A} = \sqrt{(\frac{I_{^{87}Sr}}{I_{^{86}Sr}})_{true,line\ 1} \cdot (\frac{C_{H2}}{C_{H1}}) \cdot (\frac{I_{^{87}Sr}}{I_{^{86}Sr}})_{true,line\ 2} \cdot (\frac{C_{H1}}{C_{Ax}})}$$

$$\cdot [\frac{8.375209}{(\frac{I_{^{88}Sr}}{I_{^{86}Sr}})_{true,line\ 2} \cdot (\frac{C_{H2}}{C_{Ax}})}]^{\beta_{87}}$$

$$= \sqrt{(\frac{I_{^{87}Sr}}{I_{^{86}Sr}})_{true,line\ 1} \cdot (\frac{I_{^{87}Sr}}{I_{^{86}Sr}})_{true,line\ 2}} \cdot [\frac{8.375209}{(\frac{I_{^{88}Sr}}{I_{^{86}Sr}})_{true,line\ 2}}]^{\beta_{87}}$$

$$\cdot (\frac{C_{H2}}{C_{Ax}})^{0.5-\beta_{87}} \quad (3b)$$

Therefore, ca. 99.6% of the relative cup efficiency C_{H2}/C_{Ax} is mathematically cancelled. The second multidynamic $^{87}Sr/^{86}Sr$ ratio, $(^{87}Sr/^{86}Sr)_{c,MD-B}$, was calculated using the measured $^{87}Sr/^{86}Sr$ ratios of line 2 and line 3, and the measured $^{88}Sr/^{86}Sr$ ratio of line 3:

$$(^{87}Sr/^{86}Sr)_{c,MD-B} = \sqrt{(^{87}Sr/^{86}Sr)_{m,line\ 2} \cdot (^{87}Sr/^{86}Sr)_{m,line\ 3}}$$

$$\cdot [\frac{8.375209}{(^{88}Sr/^{86}Sr)_{m,line\ 3}}]^{\beta_{87}} \quad (3c)$$

where β_{87} = 0.50359. The final multidynamic $^{87}Sr/^{86}Sr$ ratio was calculated by taking the geometric mean[31] of $(^{87}Sr/^{86}Sr)_{c,MD-A}$ and $(^{87}Sr/^{86}Sr)_{c,MD-B}$:

$$(^{87}Sr/^{86}Sr)_{c,MD} = \sqrt{(^{87}Sr/^{86}Sr)_{c,MD-A} \cdot (^{87}Sr/^{86}Sr)_{c,MD-B}} \quad (3d)$$

The fractionation-corrected static (separately for each line) or multidynamic $^{84}Sr/^{86}Sr$ and $^{87}Sr/^{86}Sr$ ratios from all cycles were averaged to derive the final measurement results of each analysed sample. The 2 standard error (2SE) values were used as the uncertainty of the averaged isotopic ratios. The overall external measurement precision of SRM 987 in the 6-month session, expressed as the 2 relative standard deviation (2RSD) value of the 43 repetitive analyses, is 36 ppm and 4.8 ppm for multidynamic $^{84}Sr/^{86}Sr$ and $^{87}Sr/^{86}Sr$ respectively.

3. Results

The $^{84}Sr/^{86}Sr$ and $^{87}Sr/^{86}Sr$ results of the 43 repetitive analyses of SRM 987 are plotted against the time of measurement (day since the beginning of the analytical session) in Fig. 1 to show their temporal variations. The static line 1 and line 2 $^{87}Sr/^{86}Sr$ ratios exhibit near-parallel decreasing trends from 0.710293 to 0.710260, and from 0.710259 to 0.710226, respectively, while the line 3 $^{87}Sr/^{86}Sr$ increases from 0.710231 to 0.710264. These long-term increasing or decreasing trends are accompanied by short-period (ca. 10 days) fluctuations. The line 1 $^{84}Sr/^{86}Sr$ increases in the first 60 days of the session from 0.056486 to 0.056496, and then remains constant throughout the rest of the session. The line 2 and line 3 $^{84}Sr/^{86}Sr$ ratios exhibit slow and slightly decreasing trends from 0.056497 to 0.056489 and 0.056494 to 0.056489, respectively, and also show some fluctuations with a ca. 50-day period. All these temporal drifts or fluctuations of static isotopic ratios are well outside the 2SE uncertainties of individual measurements. In contrast, temporal drifting is absent in the multidynamic measurement results (Fig. 1). The observed systematic changes of static Sr isotopic ratios that are not accompanied by changes in multidynamic values, thus, must reflect the changes of FCEs during the analyses of standards and unknown samples.

4. Calculation of Faraday cup deterioration degree

Our calculation method of Faraday cup deterioration degree makes use of the measurement results of SRM 987, and is based on the assumption that the observed temporal shifts in static isotopic ratios (Fig. 1) are solely caused by the changes of FCEs during the analytical session. For each multidynamic measurement of SRM 987, six static Sr isotopic ratios are obtained. They can be expressed with consideration of FCEs as (see also equation 1*c*):

$$\left({}^{87}\mathrm{Sr}/{}^{86}\mathrm{Sr}\right)_{\text{line 1}} = \left({}^{87}\mathrm{Sr}/{}^{86}\mathrm{Sr}\right)_{\text{unbiased line 1}} \cdot \mathrm{C}_{\mathrm{H2}} \cdot \mathrm{C}_{\mathrm{H1}}^{-1+\beta_{87}} \cdot \mathrm{C}_{\mathrm{H3}}^{-\beta_{87}} \quad (4a)$$

$$\left({}^{87}\mathrm{Sr}/{}^{86}\mathrm{Sr}\right)_{\text{line 2}} = \left({}^{87}\mathrm{Sr}/{}^{86}\mathrm{Sr}\right)_{\text{unbiased line 2}} \cdot \mathrm{C}_{\mathrm{H1}} \cdot \mathrm{C}_{\mathrm{Ax}}^{-1+\beta_{87}} \cdot \mathrm{C}_{\mathrm{H2}}^{-\beta_{87}} \quad (4b)$$

$$\left({}^{87}\mathrm{Sr}/{}^{86}\mathrm{Sr}\right)_{\text{line 3}} = \left({}^{87}\mathrm{Sr}/{}^{86}\mathrm{Sr}\right)_{\text{unbiased line 3}} \cdot \mathrm{C}_{\mathrm{Ax}} \cdot \mathrm{C}_{\mathrm{L1}}^{-1+\beta_{87}} \cdot \mathrm{C}_{\mathrm{H1}}^{-\beta_{87}} \quad (4c)$$

$$\left({}^{84}\mathrm{Sr}/{}^{86}\mathrm{Sr}\right)_{\text{line 1}} = \left({}^{87}\mathrm{Sr}/{}^{86}\mathrm{Sr}\right)_{\text{unbiased line 1}} \cdot \mathrm{C}_{\mathrm{L1}} \cdot \mathrm{C}_{\mathrm{H1}}^{-1+\beta_{84}} \cdot \mathrm{C}_{\mathrm{H3}}^{-\beta_{84}} \quad (4d)$$

$$\left({}^{84}\mathrm{Sr}/{}^{86}\mathrm{Sr}\right)_{\text{line 2}} = \left({}^{87}\mathrm{Sr}/{}^{86}\mathrm{Sr}\right)_{\text{unbiased line 2}} \cdot \mathrm{C}_{\mathrm{L2}} \cdot \mathrm{C}_{\mathrm{Ax}}^{-1+\beta_{84}} \cdot \mathrm{C}_{\mathrm{H2}}^{-\beta_{84}} \quad (4e)$$

$$\left({}^{84}\mathrm{Sr}/{}^{86}\mathrm{Sr}\right)_{\text{line 3}} = \left({}^{87}\mathrm{Sr}/{}^{86}\mathrm{Sr}\right)_{\text{unbiased line 3}} \cdot \mathrm{C}_{\mathrm{L3}} \cdot \mathrm{C}_{\mathrm{L1}}^{-1+\beta_{84}} \cdot \mathrm{C}_{\mathrm{H1}}^{-\beta_{84}} \quad (4f)$$

where C represents Faraday cup efficiency, $\left({}^{87}\mathrm{Sr}/{}^{86}\mathrm{Sr}\right)_{\text{unbiased}}$ and $\left({}^{84}\mathrm{Sr}/{}^{86}\mathrm{Sr}\right)_{\text{unbiased}}$ are hypothesized static isotopic ratios after fractionation correction when all FCEs are unity. Note that the "unbiased" static isotopic ratios from different lines are not necessarily equal (cf. Miyazaki et al.[35] and Makishima and Nakamura[32]) due to imperfect instrumental features other than FCE, e.g., peak shape[11] and amplifier response,[40] and we thus avoid referring to these values as the "true" or "absolute" isotopic ratios. For simplicity, the equations (4*a*–*f*) are linearized by taking natural logarithms for both sides of the equations:

$$\ln\left({}^{87}\mathrm{Sr}/{}^{86}\mathrm{Sr}\right)_{\text{line 1}} = \ln\left({}^{87}\mathrm{Sr}/{}^{86}\mathrm{Sr}\right)_{\text{unbiased line 1}} + \ln\mathrm{C}_{\mathrm{H2}} + (-1+\beta_{87}) \cdot \ln\mathrm{C}_{\mathrm{H1}} + (-\beta_{87}) \cdot \ln\mathrm{C}_{\mathrm{H3}} \quad (5a)$$

$$\ln\left({}^{87}\mathrm{Sr}/{}^{86}\mathrm{Sr}\right)_{\text{line 2}} = \ln\left({}^{87}\mathrm{Sr}/{}^{86}\mathrm{Sr}\right)_{\text{unbiased line 2}} + \ln\mathrm{C}_{\mathrm{H1}} + (-1+\beta_{87}) \cdot \ln\mathrm{C}_{\mathrm{Ax}} + (-\beta_{87}) \cdot \ln\mathrm{C}_{\mathrm{H2}} \quad (5b)$$

$$\ln\left({}^{87}\mathrm{Sr}/{}^{86}\mathrm{Sr}\right)_{\text{line 3}} = \ln\left({}^{87}\mathrm{Sr}/{}^{86}\mathrm{Sr}\right)_{\text{unbiased line 3}} + \ln\mathrm{C}_{\mathrm{Ax}} + (-1+\beta_{87}) \cdot \ln\mathrm{C}_{\mathrm{L1}} + (-\beta_{87}) \cdot \ln\mathrm{C}_{\mathrm{H1}} \quad (5c)$$

$$\ln\left({}^{84}\mathrm{Sr}/{}^{86}\mathrm{Sr}\right)_{\text{line 1}} = \ln\left({}^{84}\mathrm{Sr}/{}^{86}\mathrm{Sr}\right)_{\text{unbiased line 1}} + \ln\mathrm{C}_{\mathrm{L1}} + (-1+\beta_{84}) \cdot \ln\mathrm{C}_{\mathrm{H1}} + (-\beta_{84}) \cdot \ln\mathrm{C}_{\mathrm{H3}} \quad (5d)$$

$$\ln\left({}^{84}\mathrm{Sr}/{}^{86}\mathrm{Sr}\right)_{\text{line 2}} = \ln\left({}^{84}\mathrm{Sr}/{}^{86}\mathrm{Sr}\right)_{\text{unbiased line 2}} + \ln\mathrm{C}_{\mathrm{L2}} + (-1+\beta_{84}) \cdot \ln\mathrm{C}_{\mathrm{Ax}} + (-\beta_{84}) \cdot \ln\mathrm{C}_{\mathrm{H2}} \quad (5e)$$

$$\ln\left({}^{84}\mathrm{Sr}/{}^{86}\mathrm{Sr}\right)_{\text{line 3}} = \ln\left({}^{84}\mathrm{Sr}/{}^{86}\mathrm{Sr}\right)_{\text{unbiased line 3}} + \ln\mathrm{C}_{\mathrm{L3}} + (-1+\beta_{84}) \cdot \ln\mathrm{C}_{\mathrm{L1}} + (-\beta_{84}) \cdot \ln\mathrm{C}_{\mathrm{H1}} \quad (5f)$$

If all FCEs are invariant during a measurement and can be regarded unrelated to the intensities and angles of the incoming ion beams,[1, 23] the simultaneous equation system (5*a*–*f*) establishes the relations between the measured static isotopic ratios and the unknown FCEs, similar to the FCE measurement methods of Miyazaki et al.[35] and Makishima and Nakamura.[32] The difference between our and their methods is that our static measurement results are obtained as by-products of multidynamic measurements, while they performed separated static measurements using each cup configuration. Nonetheless, this equation system cannot be

solved for the individual FCE values, because the number of equations (i.e., the number of cup configurations or isotopes) is not enough; to solve thirteen unknowns (six "unbiased" isotopic ratios + seven FCEs), at least thirteen independent equations are needed.

The "unbiased" static isotopic ratios measured using the same instrument and the same method are usually constant over a long period of time, as evidenced by the invariant multidynamic isotopic ratios and the recovery of static isotopic ratios to their initial values when Faraday cups are renewed.[1, 10, 25, 35-37] Therefore, we can alternatively investigate *the changes of FCEs* between two measurements by taking differentials for equations (5*a–f*), assuming that the "unbiased" static isotopic ratios are constant [i.e., $\mathrm{dln}(^{87}\mathrm{Sr}/^{86}\mathrm{Sr})_{\text{unbiased line 1,2,3}} = 0$ and $\mathrm{dln}(^{84}\mathrm{Sr}/^{86}\mathrm{Sr})_{\text{unbiased line 1,2,3}} = 0$]:

$$\mathrm{dln}(^{87}\mathrm{Sr}/^{86}\mathrm{Sr})_{\text{line 1}} = \mathrm{dlnC_{H2}} + (-1+\beta_{87})\cdot\mathrm{dlnC_{H1}} + (-\beta_{87})\cdot\mathrm{dlnC_{H3}} \quad (6a)$$

$$\mathrm{dln}(^{87}\mathrm{Sr}/^{86}\mathrm{Sr})_{\text{line 2}} = \mathrm{dlnC_{H1}} + (-1+\beta_{87})\cdot\mathrm{dlnC_{Ax}} + (-\beta_{87})\cdot\mathrm{dlnC_{H2}} \quad (6b)$$

$$\mathrm{dln}(^{87}\mathrm{Sr}/^{86}\mathrm{Sr})_{\text{line 3}} = \mathrm{dlnC_{Ax}} + (-1+\beta_{87})\cdot\mathrm{dlnC_{L1}} + (-\beta_{87})\cdot\mathrm{dlnC_{H1}} \quad (6c)$$

$$\mathrm{dln}(^{84}\mathrm{Sr}/^{86}\mathrm{Sr})_{\text{line 1}} = \mathrm{dlnC_{L1}} + (-1+\beta_{84})\cdot\mathrm{dlnC_{H1}} + (-\beta_{84})\cdot\mathrm{dlnC_{H3}} \quad (6d)$$

$$\mathrm{dln}(^{84}\mathrm{Sr}/^{86}\mathrm{Sr})_{\text{line 2}} = \mathrm{dlnC_{L2}} + (-1+\beta_{84})\cdot\mathrm{dlnC_{Ax}} + (-\beta_{84})\cdot\mathrm{dlnC_{H2}} \quad (6e)$$

$$\mathrm{dln}(^{84}\mathrm{Sr}/^{86}\mathrm{Sr})_{\text{line 3}} = \mathrm{dlnC_{L3}} + (-1+\beta_{84})\cdot\mathrm{dlnC_{L1}} + (-\beta_{84})\cdot\mathrm{dlnC_{H1}} \quad (6f)$$

Replacing Faraday cup efficiencies with relative Faraday cup efficiencies (RFCE, the ratio of an FCE to the efficiency of the Axial cup, $\mathrm{C}^* \stackrel{\text{def}}{=} \mathrm{C}/\mathrm{C_{Ax}}$), equations (6*a–f*) are converted to:

$$\mathrm{dlnC^*_{H2}} + (-1+\beta_{87})\cdot\mathrm{dlnC^*_{H1}} + (-\beta_{87})\cdot\mathrm{dlnC^*_{H3}} = \mathrm{dln}(^{87}\mathrm{Sr}/^{86}\mathrm{Sr})_{\text{line 1}} \quad (7a)$$

$$\mathrm{dlnC^*_{H1}} + (-1+\beta_{87})\cdot 0 + (-\beta_{87})\cdot\mathrm{dlnC^*_{H2}} = \mathrm{dln}(^{87}\mathrm{Sr}/^{86}\mathrm{Sr})_{\text{line 2}} \quad (7b)$$

$$0 + (-1+\beta_{87})\cdot\mathrm{dlnC^*_{L1}} + (-\beta_{87})\cdot\mathrm{dlnC^*_{H1}} = \mathrm{dln}(^{87}\mathrm{Sr}/^{86}\mathrm{Sr})_{\text{line 3}} \quad (7c)$$

$$\mathrm{dlnC^*_{L1}} + (-1+\beta_{84})\cdot\mathrm{dlnC^*_{H1}} + (-\beta_{84})\cdot\mathrm{dlnC^*_{H3}} = \mathrm{dln}(^{84}\mathrm{Sr}/^{86}\mathrm{Sr})_{\text{line 1}} \quad (7d)$$

$$\mathrm{dlnC^*_{L2}} + (-1+\beta_{84})\cdot 0 + (-\beta_{84})\cdot\mathrm{dlnC^*_{H2}} = \mathrm{dln}(^{84}\mathrm{Sr}/^{86}\mathrm{Sr})_{\text{line 2}} \quad (7e)$$

$$\mathrm{dlnC^*_{L3}} + (-1+\beta_{84})\cdot\mathrm{dlnC^*_{L1}} + (-\beta_{84})\cdot\mathrm{dlnC^*_{H1}} = \mathrm{dln}(^{84}\mathrm{Sr}/^{86}\mathrm{Sr})_{\text{line 3}} \quad (7f)$$

Since $\mathrm{dln}x = \frac{\mathrm{d}x}{x}$, equations (7*a–f*) actually describe the relations of *the relative differences in static isotopic ratios* and *the relative differences in RFCEs* between two SRM 987

measurements in the analytical session. This 6-equation-6-unknown linear equation system (7*a*–*f*) can be simplified as a matrix equation $\boldsymbol{Ax} = \boldsymbol{B}$:

$$\begin{bmatrix} 0 & 0 & 0 & -1+\beta_{87} & 1 & -\beta_{87} \\ 0 & 0 & 0 & 1 & -\beta_{87} & 0 \\ 0 & 0 & -1+\beta_{87} & -\beta_{87} & 0 & 0 \\ 0 & 0 & 1 & -1+\beta_{84} & 0 & -\beta_{84} \\ 0 & 1 & 0 & 0 & -\beta_{84} & 0 \\ 1 & 0 & -1+\beta_{84} & -\beta_{84} & 0 & 0 \end{bmatrix} \begin{bmatrix} \mathrm{d}\ln C^{*}_{\mathrm{L3}} \\ \mathrm{d}\ln C^{*}_{\mathrm{L2}} \\ \mathrm{d}\ln C^{*}_{\mathrm{L1}} \\ \mathrm{d}\ln C^{*}_{\mathrm{H1}} \\ \mathrm{d}\ln C^{*}_{\mathrm{H2}} \\ \mathrm{d}\ln C^{*}_{\mathrm{H3}} \end{bmatrix} = \begin{bmatrix} \mathrm{d}\ln(^{87}\mathrm{Sr}/^{86}\mathrm{Sr})_{\mathrm{line1}} \\ \mathrm{d}\ln(^{87}\mathrm{Sr}/^{86}\mathrm{Sr})_{\mathrm{line2}} \\ \mathrm{d}\ln(^{87}\mathrm{Sr}/^{86}\mathrm{Sr})_{\mathrm{line3}} \\ \mathrm{d}\ln(^{84}\mathrm{Sr}/^{86}\mathrm{Sr})_{\mathrm{line1}} \\ \mathrm{d}\ln(^{84}\mathrm{Sr}/^{86}\mathrm{Sr})_{\mathrm{line2}} \\ \mathrm{d}\ln(^{84}\mathrm{Sr}/^{86}\mathrm{Sr})_{\mathrm{line3}} \end{bmatrix} \quad (8)$$

Equation (8) has a theoretical unique solution $\boldsymbol{x} = \boldsymbol{A}^{-1}\boldsymbol{B}$ if and only if the coefficient matrix's determinant $|\boldsymbol{A}| = \beta_{84} - 2\beta_{84}\cdot\beta_{87} + \beta_{84}\cdot\beta_{87}^2 + \beta_{87}^2 \neq 0$. However, when β_{84} and β_{87} are replaced with the exponential law fractionation exponents $\beta_{84} = -1.02325$ and $\beta_{87} = 0.50359$, the coefficient matrix $\boldsymbol{A}$ becomes ill-conditioned with a near-zero determinant $|\boldsymbol{A}| = 0.00145$ and a huge condition number of 9.8×10^3 (condition number is calculated as $\|\boldsymbol{A}\|_\infty \cdot \|\boldsymbol{A}^{-1}\|_\infty$, where $\|\cdot\|_\infty$ represents the ∞-norm of a matrix).[41] A square matrix's condition number theoretically represents the maximum ratio of the relative error in the solution vector $\boldsymbol{x}$ (measured using matrix norm) to the relative error in the constant vector $\boldsymbol{B}$. This high condition number of the matrix $\boldsymbol{A}$ reflects the high sensitivity of the solution $\boldsymbol{x}$ of equation (8) to the small perturbations in the constant vector $\boldsymbol{B}$, so that any error in $\boldsymbol{B}$ will result in a much larger relative error (magnified by a factor up to 9.8×10^3) in $\boldsymbol{x}$. This significant error magnification is a property of the ill-conditioned equation system but is not related to measurement or calculation errors. Attempts to solve equation (8) with consideration of the measurement uncertainties in $\boldsymbol{B}$ (typically 10^{-6}–10^{-5}) using a Monte Carlo method yielded typical uncertainties of 10^{-3} to 10^{-2} for $\boldsymbol{x}$, making the relative changes in RFCE smaller than 1000 ppm difficult to resolve. Per mil-level deviations of RFCEs were observed in older-generation mass spectrometers,[27-30, 32] but this effect seems much reduced (e.g., to 10–100 ppm level) in modern TIMS instruments[35, 42] probably owing to better designed Faraday cups and ion optics.[1, 9, 25] Therefore, though

mathematically correct, the equations (7*a*–*f*) cannot provide precise constraints on small-degree Faraday cup deteriorations.

The almost singular coefficient matrix $\boldsymbol{A}$ reflects that some equation(s) in (7*a*–*f*) is not completely independent. We noticed that the left hand side of equation (7*d*) is approximately a linear combination of the left hand sides of equations (7*a*–*c*). Therefore, we removed (7*d*) from the equation system to achieve better equation independence and solving precision. To solve the remaining 5-equation-6-unknown system, another independent constraint of the relative differences of RFCEs is needed. Below we show that an independent constraint can be established by taking the advantage of the unique characteristic of the isotope system of Sr.

The efficiency of a Faraday cup reflects its ability to prevent the generation and escape/entry of secondary charged particles when the ion beam hits the cup. Though the physical mechanism of Faraday cup inefficiency is not completely understood, it is believed to be a synthetic effect related to the geometry and physical properties of the cup, the amount, chemistry, topography, and distribution of coating materials in the cup liner, as well as the intensity and incidence angle of the incoming ion beam.[1, 22, 23, 28] Nonetheless, a primary parameter controlling the Faraday cup efficiency is likely the amount of accumulated measured elements inside the cup and the associated changes of surface properties, e.g., secondary particle yield.[1] During the 6-month analytical session, our Triton *Plus* TIMS was exclusively used for Sr isotope analyses of various natural samples and reference materials, using either the multidynamic method described in this paper or a static method equivalent to its line 1 (without idle time, and zoom optics set at zero). The sample (Sr) amounts of the static runs were generally 5–10 times smaller than those of the multidynamic runs. Rubidium and molecular interferences were negligible in all the measurements. Given this simple instrument usage scheme, the number of Sr atoms deposited in the cups during this session should strictly correspond to the cup configurations used for the measurements, and thus can be quantitatively

353 estimated using the measured intensity data. Particularly, we noticed that in the multidynamic
354 method shown in Table 1, the cups L2 and L3 have a "symmetric" status; they are equally used
355 to collect only ^{84}Sr ions in the line 2 or line 3 of the multidynamic runs respectively, while
356 other cups are used to collect different combinations of Sr isotopes from both static and
357 multidynamic runs (^{84}Sr + ^{86}Sr for L1, ^{86}Sr + ^{87}Sr for Ax, ^{86}Sr + ^{87}Sr + ^{88}Sr for H1,^{87}Sr + ^{88}Sr
358 for H2, and ^{88}Sr for H3). Therefore, in a multidynamic measurement cycle, if the ion beam
359 intensities are relatively stable, and no significant truncation loss of ions occurs at the cup
360 entrances, the cups L2 and L3 should always collect equal (and relatively small) amounts of
361 ^{84}Sr ions. Actually, when the ion beam intensities are increasing during the heating stage at the
362 beginning of measurements, the time-integrated amount of ^{84}Sr ions deposited in L3 may be
363 slightly more than that in L2. However, this stage is relatively short compared to the entire
364 measurement, and the intensities are relatively low, so this effect can be compensated to some
365 extent at later stages when the ion beam intensities are decreasing (e.g., at the end of the
366 measurement). Ion beam truncation may occur due to imperfect peak alignment or optic
367 aberration, but this can be recognized by anomalous peak and/or baseline shapes,[5, 31, 43] which
368 were never seen throughout our measurements. In the static measurements, no ions are
369 introduced into the cups L2 and L3. Therefore, after each complete standard or sample
370 measurement (no matter static or multidynamic), the cups L2 and L3 should always have
371 received approximately equal amounts of ^{84}Sr deposition, and thus should have deteriorated by
372 equal degrees, under the assumption that the accumulation of Sr atoms in the cup is the sole
373 cause of cup deterioration. This inference brings in a new independent constraint on the relative
374 differences of RFCEs between two SRM 987 measurements in our session: $\mathrm{dln}C^*_{L3} = \mathrm{dln}C^*_{L2}$.
375 Applying the assumption $\mathrm{dln}C^*_{L3} = \mathrm{dln}C^*_{L2}$, the matrix equation (8) is reduced to:

$$\begin{bmatrix} 0 & 0 & -1+\beta_{87} & 1 & -\beta_{87} \\ 0 & 0 & 1 & -\beta_{87} & 0 \\ 0 & -1+\beta_{87} & -\beta_{87} & 0 & 0 \\ 1 & 0 & 0 & -\beta_{84} & 0 \\ 1 & -1+\beta_{84} & -\beta_{84} & 0 & 0 \end{bmatrix} \begin{bmatrix} d\ln C^{*}_{L2} \\ d\ln C^{*}_{L1} \\ d\ln C^{*}_{H1} \\ d\ln C^{*}_{H2} \\ d\ln C^{*}_{H3} \end{bmatrix} = \begin{bmatrix} d\ln(^{87}Sr/^{86}Sr)_{line1} \\ d\ln(^{87}Sr/^{86}Sr)_{line2} \\ d\ln(^{87}Sr/^{86}Sr)_{line3} \\ d\ln(^{84}Sr/^{86}Sr)_{line2} \\ d\ln(^{84}Sr/^{86}Sr)_{line3} \end{bmatrix} \quad (9)$$

The coefficient matrix of equation (9) has a smaller condition number of 117, suggesting that it may be possible to resolve Faraday cup deterioration at 10–100 ppm level. Replace β_{84} and β_{87} with –1.02325 and 0.50359, the solution to equation (9) is:

$$\begin{bmatrix} d\ln C^{*}_{L2} \\ d\ln C^{*}_{L1} \\ d\ln C^{*}_{H1} \\ d\ln C^{*}_{H2} \\ d\ln C^{*}_{H3} \end{bmatrix} = \begin{bmatrix} 0 & 5.98712 & 7.93367 & 2.94655 & -1.94655 \\ 0 & 1.9747 & 1.94655 & 0.971845 & -0.971845 \\ 0 & -1.94655 & -3.90454 & -0.957989 & 0.957989 \\ 0 & -5.85109 & -7.75341 & -1.90232 & 1.90232 \\ -1.98574 & -9.69995 & -11.5474 & -2.83319 & 2.83319 \end{bmatrix} \begin{bmatrix} d\ln(^{87}Sr/^{86}Sr)_{line1} \\ d\ln(^{87}Sr/^{86}Sr)_{line2} \\ d\ln(^{87}Sr/^{86}Sr)_{line3} \\ d\ln(^{84}Sr/^{86}Sr)_{line2} \\ d\ln(^{84}Sr/^{86}Sr)_{line3} \end{bmatrix} \quad (10)$$

Using equation (10), one can calculate the relative differences of RFCEs between two multidynamic SRM 987 measurements from the observed relative differences of their static Sr isotopic ratios. The uncertainties of the calculated relative differences of RFCEs can be easily evaluated using the general error propagation method, such as that described by Makishima and Nakamura.[32]

5. Discussion

5.1 Faraday cup deterioration during this study

Within our analytical session, if one SRM 987 measurement is selected as the reference point and all other SRM 987 measurements are used to calculate RFCE differences relative to this common reference, the continuous changes of RFCEs (i.e., Faraday cup deterioration) can be tracked. Here, the first SRM 987 measurement performed at the beginning of our session is selected as the reference (i.e., initial status), and thus the cup deterioration degrees at this initial status relative to themselves are zeroes by definition. Following the method described in section 4, we calculated the relative changes of RFCEs of the 6 Faraday cups (Table 1, except

the Axial cup which is used as the reference cup in the definition of RFCE) relative to their initial status using all the 43 multidynamic SRM 987 measurements performed in the session, and show the calculation results in Fig. 2b–f. In these figures, bin-average smoothing curves of the data points and their standard deviation ranges, computed using a bootstrapping method (described in the caption to Fig. 2) with the uncertainties of individual data points considered, are also plotted to quantitatively show the variation trends of the cup deterioration degrees. During our analytical session, the low-mass cups L1, L2, and L3 do not exhibit resolvable deterioration (Fig. 2b, c). In contrast, the RFCEs of the high-mass cups have significantly changed relative to their initial status (Fig. 2d–f). Most of these efficiency changes occurred in the first 60 days of the session; the RFCE of cup H1 decreased by ca. 80 ppm, while the RFCEs of H3 and H2 experienced increases (by 150 ppm and 50 ppm respectively) followed by decreases (by 150 ppm and 100 ppm respectively). The RFCEs of the three high-mass cups then became stable in the rest of the session, with a slight downward kink at days 160–170. The observed temporal variation trends of the deterioration degrees of the high-mass cups described above are tested to be significant time-series signals different from noises (of which the mean values do not change over time) associated with random scattering of data points. Two methods that have been used to quantitatively resolve these signals from random noises, "uniformity of multiple time scales" and "autocorrelation function", are described in the Electronic Supplementary Information in detail. The occurrences of the RFCE changes also temporally coincide the drifts of the static Sr isotopic ratios shown in Fig. 1.

As has been discussed above, a primary parameter controlling FCE change is likely the amount of accumulated measured elements inside the cup and the associated changes of surface properties.[1, 25] The simple single-element usage scheme of our instrument during the analytical session suggests that we can quantify the accumulation of Sr atoms in the Faraday cups, and examine its relation with the observed Faraday cup deterioration trends. We compiled all the

static and multidynamic Sr isotope analyses performed during this session, and calculated the amounts of Sr atoms deposited in the Faraday cups during each measurement by integrating the measured ion beam intensities. Because the data collection in almost all the measurements started immediately when small signals appeared and stopped after the samples were completely exhausted, the integrated Sr atom numbers using the acquired data are to the utmost extents close to the true amounts of Sr ions delivered into the Faraday cups. Fig. 2a shows the accumulated amounts of Sr atoms in the cups along with time since the beginning of the session. The accumulated amounts of Sr atoms in all the cups increased linearly in an approximately proportional manner. At the end of the analytical session, the cups H1, H2, and H3 have accumulated 5–142 times more Sr atoms than other cups. This can be easily explained by the cup configuration shown in Table 1; the cups H1, H2, and H3 were used to collect ^{88}Sr, the most abundant isotope of Sr. In contrast, the cups L2 and L3 were only used to collect the least abundant isotope ^{84}Sr, and as a result, the accumulation of Sr atoms in these two cups is small compared to other cups.

The substantial deposition of Sr atoms in the cups H1, H2, H3 during the analytical session is broadly consistent with only these three cups showing resolvable efficiency changes (Fig. 2d–f). This confirms that the massive accumulation of measured elements in the cups can effectively alter Faraday cup efficiencies. However, the exact response function of cup efficiency to the accumulation of Sr atoms in the cups, as seen in Fig. 3, is far from monotonic or linear. Though the accumulated amounts of Sr atoms in the three high-mass cups define monotonic, near-linear increasing trends during the session (Fig. 2a), these cups exhibit complex efficiency change patterns with both increasing and decreasing periods as the Sr atom number in the cups increases (Figs. 2d–f and 3). Furthermore, the responses of different cups to the same amount of deposition of Sr atoms can differ in magnitude and sometimes direction (Fig. 3). This suggests that Faraday cup deterioration is not a simple univariate function of the

accumulation of measured elements. Other factors, such as the deterioration history of individual cups and the change of surface roughness caused by different coating elements,[22] may also play important roles in the direction and degree of cup efficiency change. Since the installation in 2010, our Triton *Plus* has been mainly used for isotopic analyses of Sr, Nd, and Pb in static multi-collection mode. The Faraday cups were never refreshed in the 9-year usage history. Different ion exposure history and stage of life of the cups may explain the observed divergence of the static $^{87}Sr/^{86}Sr$ and $^{84}Sr/^{86}Sr$ ratios at the beginning of the session (Fig. 1) as well as the different responses of cup efficiency to the deposition of Sr atoms (Fig. 3). This indication appears contradictory to our assumption introduced in section 4 that the cups L2 and L3 have equal deterioration degrees (i.e., $\mathrm{dln}C^*_{L3} = \mathrm{dln}C^*_{L2}$) as the consequence of their equal increments of Sr accumulation between measurements. Assuming that L2 and L3 have different deterioration responses to the increase of Sr atoms in the cups: $\mathrm{dln}C^*_{L3} = F_{L3} \cdot \mathrm{d}Sr_{L3}$ and $\mathrm{dln}C^*_{L2} = F_{L2} \cdot \mathrm{d}Sr_{L2}$ where F is a variable responding factor, when $\mathrm{d}Sr_{L3} = \mathrm{d}Sr_{L2} = \mathrm{d}Sr$, we have: $\mathrm{dln}C^*_{L3} - \mathrm{dln}C^*_{L2} = (F_{L3} - F_{L2}) \cdot \mathrm{d}Sr$. Valid application of this assumption (i.e., $\mathrm{dln}C^*_{L3} - \mathrm{dln}C^*_{L2} = 0$) thus requires either $F_{L3} = F_{L2}$ or $\mathrm{d}Sr = 0$. During our analytical session, only the least abundant isotope of Sr, ^{84}Sr, was directed into the cups L2 and L3. The atomic abundance of ^{84}Sr is only 0.56%,[39] which is 12–147 times lower than other isotopes of Sr (^{87}Sr, ^{86}Sr, ^{88}Sr). Therefore, the increase of Sr atoms in the cups L2 and L3 can be regarded negligible relative to that in other cups (i.e., $\mathrm{d}Sr = 0$ can be regarded reasonable), and $F_{L3} = F_{L2}$ is not required in our calculation. As also shown in section 5.3 quantitatively, we argue that this conclusion does not invalidate our FCE deterioration degree calculation method described in section 4.

5.2 Comparison with existing FCE measurement methods

A number of methods have been previously developed to quantitatively measure FCEs (or RFCEs) on MC–TIMS and MC–ICPMS. The most straightforward way to measure RFCEs

is the single isotope cup jumping method, in which an ion beam is sequentially measured using the Faraday cup of interest and a reference cup (usually the Axial cup) by changing magnetic field, and then RFCE is calculated as their intensity ratio. Though fractionation need not be considered, this method obviously requires an ion beam with exceptional short-term and long-term stability, and accurate modelling and interpolation of small long-term variations (same as in isotope ratio measurements by single collector peak-jumping).[1, 28-30] This can be difficult to achieve in either TIMS or ICPMS ion sources. The bilinear interpolation method described by Wendt and Haase[29] can largely reduce the uncertainties associated with the temporal drift of ion beam intensity, but the measurement precision of RFCE is still limited by the intensity and stability of ion currents. Another method, first developed by Makishima and Nakamura[32] and modified by Kimura et al.[44] and Miyazaki et al.,[35] uses the exponential law- (or power law-) corrected static isotopic ratios measured using different Faraday cup combinations to calculate RFCEs. With this method, it is possible to simultaneously solve $N - 1$ ($N \geq 4$) RFCEs plus one true isotopic ratio (assumed to be constant) using the static measurement results from at least N different cup configurations. The drawback of this method is that it requires a series of static multi-collection measurements using different cup configurations with mandatory physical movements of Faraday cups. Based on similar principles, Albarède et al.[5] formulated matrix equations for multidynamic MC–ICPMS measurements to simultaneously solve RFCEs, fractionation degrees, and true isotopic ratios. However, their equation systems (54) and (55) are apparently underdetermined because the coefficient matrices are rank-deficient. Therefore, their solutions to RFCEs may not be unique. A simpler and more efficient method was recently developed by Davis[42] to measure multiple RFCEs using only two measurement sequences with one reconfiguration of Faraday cups and magnetic field in between. However, the applicability and efficiency of this method vary with the number of isotopes of the chosen isotopic system (e.g., three RFCEs can be simultaneously determined using Nd each time, while only one

RFCE can be obtained using Sr). Besides, not all Faraday cups installed in the instrument can be characterized by this method; the two outermost cups are always beyond reach because they are used to monitor mass fractionation.

Most of the RFCE measurement methods summarized above require additional, specially designed experiments which cannot be easily and frequently performed within the routine isotopic analyses of standards and unknown samples in the laboratory. The only exception, the single isotope cup jumping method, however, is severely limited by the requirement of exceptionally good ion beam stability. Unlike these existing methods, our new method enables continuous and quantitative tracking of individual cup deterioration trends using only routinely analysed laboratory standards without separate, sophisticated experiments. The analyses of reference standards and screening of cup efficiency deterioration can be achieved simultaneously. It should be noted, however, that only the relative changes of RFCEs between measurements, not the absolute RFCE values, are obtained using the calculation method described here. This new method is by no means a substitution to the direct methods for RFCE determination and calibration,[28, 32, 35, 42] but is a simpler approach to quantitatively monitor the degree and direction of Faraday cup deterioration within an analytical session.

5.3 Reliability and applicability of our method

Our calculation method of cup deterioration degrees is based on four assumptions: (1) RFCEs are constant during a measurement, i.e., they are not dependent on the incidence location, angle and intensity of the incoming ion beams; (2) instrumental mass fractionation can be accurately described using the exponential law, and the β values used are correct; (3) "unbiased" static isotopic ratios of the standard are invariant between measurements; and (4) the relative changes of RFCEs of cups L3 and L2 are equal between measurements. The first three assumptions are the same as in the previous methods developed by Makishima and Nakamura[32] and Miyazaki et al,[35] and also form the basis of any multidynamic isotope analyses.

The last assumption is critical to make the equation system (9) solvable without adding more cup configurations, and its reliability needs to be assessed. This assumption is rigorously valid at the most ideal situation when the change of RFCE is a linear function of the accumulated amount of Sr atoms in the cup, and the cups L3 and L2 always receive equal amounts of Sr deposition in each measurement. We have no a priori knowledge about the response function of RFCE to the deposition of analysed elements, and furthermore, the observed responses (Fig. 3) do not support a linear relation. However, we can evaluate the effect when $\mathrm{dln}C^*_{L3} \neq \mathrm{dln}C^*_{L2}$ by assigning an uncertainty to $\mathrm{dln}C^*_{L3} - \mathrm{dln}C^*_{L2}$, and propagating this uncertainty into the final solution of equation (9). In our previous calculations, the value of $\mathrm{dln}C^*_{L3} - \mathrm{dln}C^*_{L2}$ was assumed to be zero without any uncertainty. Our repetitive calculations show that even if an extreme uncertainty of $\pm 5\times10^{-5}$ (the observed maximal variation range of $\mathrm{dln}C^*_{L3}$ and $\mathrm{dln}C^*_{L2}$ during the session is ca. 1×10^{-4}) is assigned to $\mathrm{dln}C^*_{L3} - \mathrm{dln}C^*_{L2}$, the drifting trends in $\mathrm{dln}C^*_{H3}$ and $\mathrm{dln}C^*_{H1}$ shown in Fig. 2 are still resolvable. Therefore, our calculations of Faraday cup deterioration degrees are reliable as long as the differences between $\mathrm{dln}C^*_{L3}$ and $\mathrm{dln}C^*_{L2}$ between measurements do not exceed 100 ppm.

The equation (7*d*) was excluded in our previous calculation of relative differences of RFCEs. Therefore, it provides an independent way to check the reliability of our calculation results. Using the solved relative differences of RFCEs between measurements by equation (10), if the calculated residue between the left and right hand sides of the equation (7*d*) equals zero within error, our calculation results can be regarded self-consistent. As shown in Fig. 4, using the solved relative differences of RFCEs of cups L1, H1, and H3 and the measured relative differences of $(^{84}Sr/^{86}Sr)_{\text{line 1}}$ between each SRM 987 measurement and the first SRM 987 measurement in the analytical session, the residues of equation (7*d*) of almost all our SRM 987 measurements are indistinguishable from zero, supporting that our estimations of the relative changes of RFCEs (Fig. 2) are reliable.

Our quantitative calculation method of Faraday cup deterioration degrees can potentially be applied to other isotopic analyses and other types of MC mass spectrometers. A generalized procedure for such calculation is as follows (a flow chart is provided in the Electronic Supplementary Information): (1) in a specific analytical session, perform regular multidynamic isotope analyses for reference standards together with the analyses of unknown samples; (2) for the analyses of the standard, write the equations for all possible static isotopic ratios (similar to our equations 4*a*–*f*). Linearize and differentiate both sides of the equations. Select the linearly independent equations out of them and derive a $n \times n$ matrix equation similar to our equation (8); (3) solve the matrix equation using the standard data with uncertainties propagated; (4) if the matrix equation does not have a unique solution, or the uncertainty of the solution is significantly magnified (like in this study), introduce additional independent constraints about the cup deterioration degrees. These constraints can be established based on the characteristics of the analysed isotopic system (such as $\mathrm{d}\ln C^{*}_{L3} = \mathrm{d}\ln C^{*}_{L2}$ in this study). For the elements that, like Sr, contain at least one low-abundance isotope (e.g., Ca, Ba, W, Pb, Cr), assumptions similar to ours may be directly applicable. In the cases where none of the isotopes of the analysed element can be readily regarded negligible (such as Nd), the effect of responding factor (*F*) discussed in section 5.1 may be important. If *F* is highly different between cups, the relation between the deterioration degrees of the cups cannot be easily inferred from the amounts of atom deposition. In such a situation, the magnitude of the difference in *F*, and whether it has a significant effect on cup deterioration, require careful evaluation; (5) if no additional independent constraint is available or achievable, more cup configurations have to be added[32, 35] to establish new independent constraints about cup deterioration degrees. Cup efficiency characterization is more straightforward if other elements are not introduced into the cups during the analytical session. In this case, the complex

570 superposition and interaction of deterioration effects caused by different elements can be
571 avoided.

572 *5.4 Potential application to MC-SIMS and MC-ICPMS*

573 The effect of FCE (and detector efficiency in general), though theoretically a common
574 issue for all MC mass spectrometers, has been rarely discussed in literature for mass
575 spectrometer types other than TIMS, e.g., ICPMS and SIMS. This, in our opinion, can be
576 attributed to two reasons: (1) the effect is seen as generally insignificant compared to the
577 measurement uncertainty; and (2) in MC–ICPMS and MC–SIMS measurements, reference
578 standards are frequently analysed between unknown samples to monitor the instrument
579 stability, or the sample–standard bracketing method is used to correct instrument mass biases,
580 so that any detector efficiency differences are cancelled out immediately during analyses.
581 However, many MC–ICPMS measurements also use other methods for mass bias correction,
582 such as internal normalization, element doping, and double spike.[4] Detector efficiencies cannot
583 be eliminated by these methods. MC–ICPMS analyses are now achieving ppm-level precision
584 similar to MC–TIMS. It is also foreseeable that the measurement precision of MC–SIMS will
585 reach the similar level in the near future owing to the rapid technical improvements. As a
586 consequence, the previously insignificant detector efficiency issues in MC–ICPMS and MC–
587 SIMS are likely to become a substantial component of total measurement uncertainty.

588

589 **6. Conclusion**

590 We have presented a method based on solving linear equation system to calculate the
591 changes of relative Faraday cup efficiencies (RFCEs) between multidynamic analyses of
592 reference standards using the measured relative changes of their static isotopic ratios. This
593 method can be used to quantitatively and continuously track Faraday cup deterioration during
594 routine isotope analyses without specially designed experiments. Using this method, significant

Faraday cup deteriorations (up to 150 ppm) were observed during a 6-month Sr isotope analytical session. The most heavily deteriorated cups were the same ones which have received the most abundant Sr atom deposition, confirming that the accumulation of measured elements can effectively alter Faraday cup efficiencies. The observed response function of cup efficiency to the accumulation of Sr atoms in the cup is complex and non-linear, and differs between cups in magnitude and direction, suggesting that Faraday cup deterioration is not a simple univariate function of the accumulation of measured elements. Other factors, such as the exposure history to the ion beams of other elements, may also play important roles in the direction and degree of cup efficiency change.

Conflicts of interest

There are no conflicts to declare.

Acknowledgements

We thank Evgenii Krestianinov and Sonja Zink for help with the Sr isotope analyses, and Marc Norman and Richard Armstrong for providing the statically measured Sr isotope data used for the evaluation of ion accumulation in Faraday cups. This project was funded through the Australian Research Council grant DP190100002 “The history of accretion in our Solar System”. We thank two anonymous reviewers for comments on the manuscript.

Tables

Table 1 Cup configuration of the multidynamic TIMS method used in this study.

Cup	L3	L2	L1	Ax	H1	H2	H3	Zoom optics		Integration time (s)	Idle time (s)
Amplifier (Ω)[a]	10^{11}	10^{11}	10^{11}	10^{11}	10^{11}	10^{11}	10^{11}	Focus (V)	Dispersion (V)		
Line 1			^{84}Sr	^{85}Rb	^{86}Sr	^{87}Sr	^{88}Sr	–2	8	8.389	3.000
Line 2		^{84}Sr	^{85}Rb	^{86}Sr	^{87}Sr	^{88}Sr		0	0	8.389	3.000
Line 3	^{84}Sr	^{85}Rb	^{86}Sr	^{87}Sr	^{88}Sr			2	–8	8.389	3.000

[a] Amplifier rotation: “left”

Figures and captions

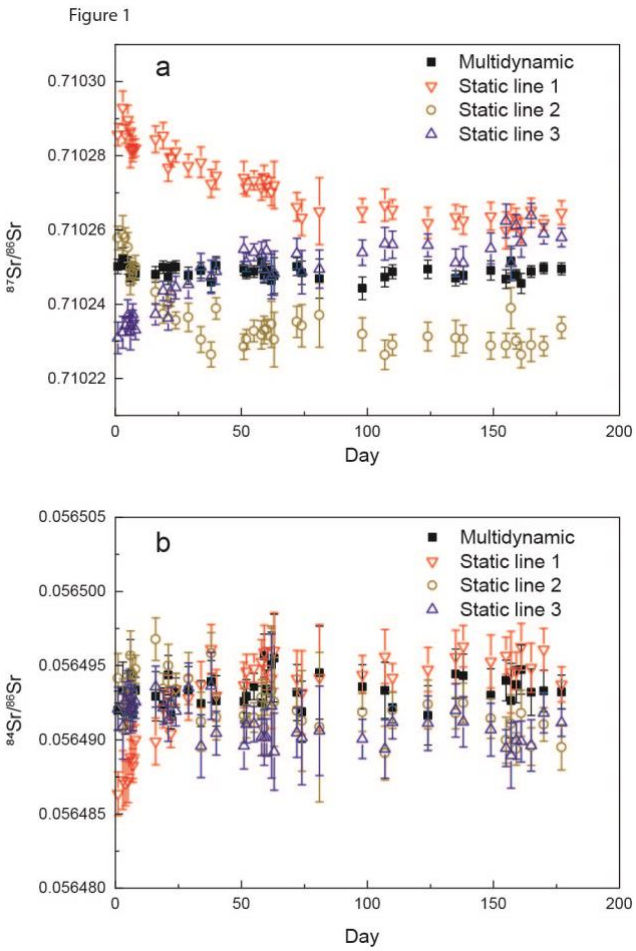

Figure 1. $^{87}Sr/^{86}Sr$ and $^{84}Sr/^{86}Sr$ measurement results of the standard SRM 987, plotted against the time of measurement (day since the beginning of the analytical session). (a): Static and multidynamic $^{87}Sr/^{86}Sr$ ratios; (b): static and multidynamic $^{84}Sr/^{86}Sr$ ratios.

Figure 2

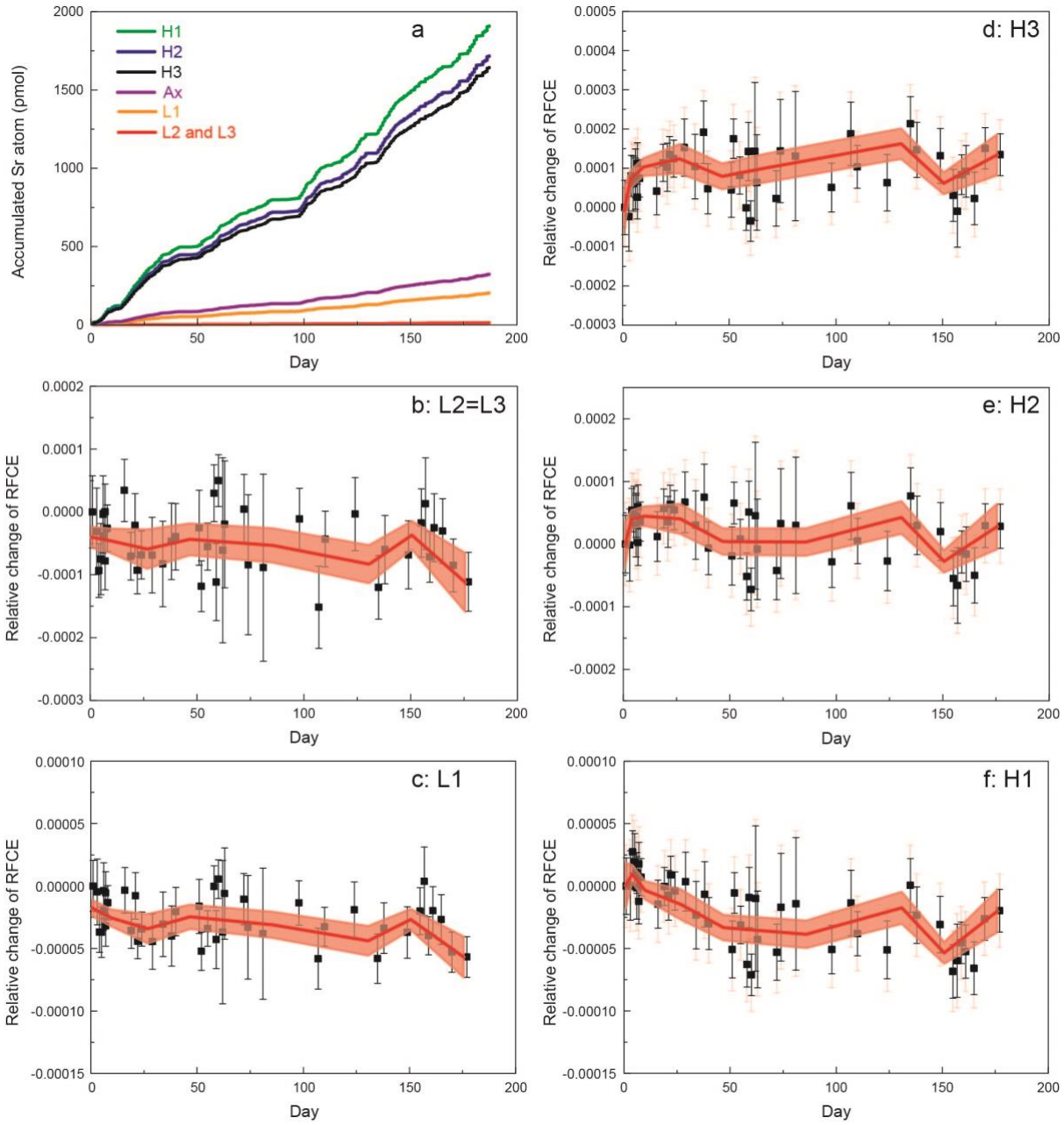

Figure 2. (a): Accumulated amounts of Sr atoms in the Faraday cups since the beginning of the analytical session, calculated using all the static and multidynamic Sr isotope analyses performed during the session. (b)–(f): Relative changes of relative Faraday cup efficiencies (RFCEs) compared to their initial status at the beginning of the analytical session (i.e., dlnC* values in equation 8), calculated using the 43 SRM 987 measurements performed in the analytical session. Black error bars represent standard errors of the relative changes of RFCEs

under the assumption that the cups L2 and L3 have equal RFCE changes between two measurements (i.e., $\mathrm{dln}C^{*}_{L3} = \mathrm{dln}C^{*}_{L2}$; see section 4 for details). In (d)–(f), the red error bars represent standard errors of the relative changes of RFCEs when the difference between $\mathrm{dln}C^{*}_{L3}$ and $\mathrm{dln}C^{*}_{L2}$ has an uncertainty of 5×10^{-5} (i.e., $\mathrm{dln}C^{*}_{L3} - \mathrm{dln}C^{*}_{L2} = 0 \pm 5 \times 10^{-5}$). Red curves and bands in (b)–(f) are bin-average smoothing curves of the data points and their standard deviation ranges, computed using a bootstrapping resampling method. In each resampling, a series of new data points are randomly generated *in situ* from the normal distribution of each real data point, with the corresponding standard error as standard deviation. The randomly generated data points are averaged within a number of manually-separated bins. The mean and standard deviation of each bin average value are calculated by 1000 times of random resampling.

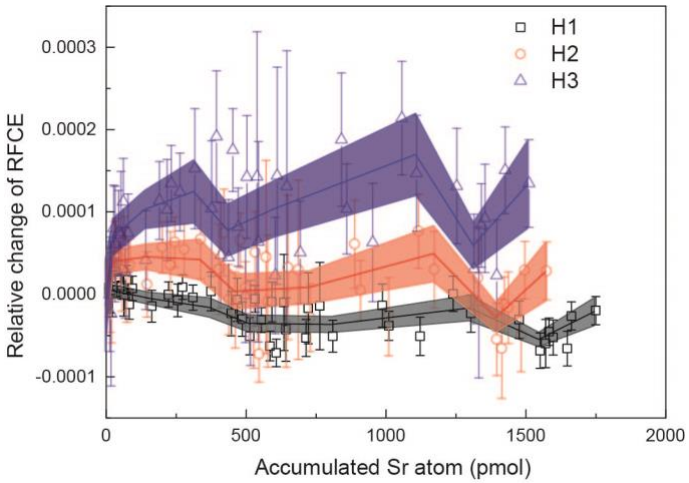

Figure 3. Responses of RFCEs to the increase of Sr atom in Faraday cups. Relative changes of RFCEs of the cups H1, H2, H3, same as in Fig. 2d–f, are plotted against the accumulated amount of Sr atoms in those cups from Fig. 2a. Bin-average smoothing curves of the data points and their standard deviation ranges are plotted using the same approach as in Fig. 2.

Figure 4

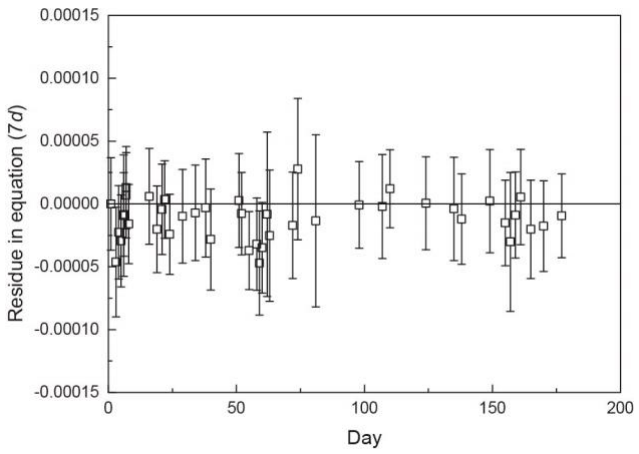

Figure 4. Residues of equation (7*d*) of the SRM 987 measurements in our analytical session plotted against the time when the measurement was made (day since the beginning of the analytical session). Residues are calculated as the left hand side of equation (7*d*) minus the right hand side. Uncertainties are 2SE.

References

1. R. W. Carlson, 15.18 - Thermal Ionization Mass Spectrometry, in *Treatise on Geochemistry (Second Edition)*, eds. H. D. Holland and K. K. Turekian, Elsevier, Oxford, 2014, pp. 337-354.
2. A. Makishima, *Thermal Ionization Mass Spectrometry (TIMS): Silicate Digestion, Separation, and Measurement*, John Wiley & Sons, Weinheim, Germany, 2016.
3. J. W. Olesik, 15.17 - Inductively Coupled Plasma Mass Spectrometers, in *Treatise on Geochemistry (Second Edition)*, eds. H. D. Holland and K. K. Turekian, Elsevier, Oxford, 2014, DOI: https://doi.org/10.1016/B978-0-08-095975-7.01426-1, pp. 309-336.
4. L. Yang, Accurate and precise determination of isotopic ratios by MC-ICP-MS: A review, *Mass Spectrometry Reviews*, 2009, **28**, 990-1011.

5. F. Albarède, P. Telouk, J. Blichert-Toft, M. Boyet, A. Agranier and B. Nelson, Precise and accurate isotopic measurements using multiple-collector ICPMS, *Geochimica et Cosmochimica Acta*, 2004, **68**, 2725-2744.

6. N. Jakubowski, T. Prohaska, L. Rottmann and F. Vanhaecke, Inductively coupled plasma- and glow discharge plasma-sector field mass spectrometry Part I. Tutorial: Fundamentals and instrumentation, *J. Anal. At. Spectrom.*, 2011, **26**, 693-726.

7. R. Arevalo, 15.23 - Laser Ablation ICP-MS and Laser Fluorination GS-MS, in *Treatise on Geochemistry (Second Edition)*, eds. H. D. Holland and K. K. Turekian, Elsevier, Oxford, 2014, DOI: https://doi.org/10.1016/B978-0-08-095975-7.01432-7, pp. 425-441.

8. T. R. Ireland, 15.21 - Ion Microscopes and Microprobes, in *Treatise on Geochemistry (Second Edition)*, eds. H. D. Holland and K. K. Turekian, Elsevier, Oxford, 2014, DOI: https://doi.org/10.1016/B978-0-08-095975-7.01430-3, pp. 385-409.

9. M. E. Wieser and J. B. Schwieters, The development of multiple collector mass spectrometry for isotope ratio measurements, *Int. J. Mass Spectrom.*, 2005, **242**, 97-115.

10. M. Garçon, M. Boyet, R. W. Carlson, M. F. Horan, D. Auclair and T. D. Mock, Factors influencing the precision and accuracy of Nd isotope measurements by thermal ionization mass spectrometry, *Chemical Geology*, 2018, **476**, 493-514.

11. E. Yobregat, C. Fitoussi and B. Bourdon, A new method for TIMS high precision analysis of Ba and Sr isotopes for cosmochemical studies, *J. Anal. At. Spectrom.*, 2017, **32**, 1388-1399.

12. G. J. Archer, A. Mundl, R. J. Walker, E. A. Worsham and K. R. Bermingham, High-precision analysis of $^{182}W/^{184}W$ and $^{183}W/^{184}W$ by negative thermal ionization mass

spectrometry: Per-integration oxide corrections using measured $^{18}O/^{16}O$, *Int. J. Mass Spectrom.*, 2017, **414**, 80-86.

13. A. Trinquier, J.-L. Birck and C. J. Allègre, High-precision analysis of chromium isotopes in terrestrial and meteorite samples by thermal ionization mass spectrometry, *J. Anal. At. Spectrom.*, 2008, **23**, 1565-1574.

14. M. Bizzarro, C. Paton, K. Larsen, M. Schiller, A. Trinquier and D. Ulfbeck, High-precision Mg-isotope measurements of terrestrial and extraterrestrial material by HR-MC-ICPMS—implications for the relative and absolute Mg-isotope composition of the bulk silicate Earth, *J. Anal. At. Spectrom.*, 2011, **26**, 565-577.

15. Q.-F. Mei, J.-H. Yang and Y.-H. Yang, An improved extraction chromatographic purification of tungsten from a silicate matrix for high precision isotopic measurements using MC-ICPMS, *J. Anal. At. Spectrom.*, 2018, **33**, 569-577.

16. N. Dauphas, S. G. John and O. Rouxel, Iron Isotope Systematics, *Reviews in Mineralogy and Geochemistry*, 2017, **82**, 415-510.

17. M. Chaussidon, Z. Deng, J. Villeneuve, J. Moureau, B. Watson, F. Richter and F. Moynier, In Situ Analysis of Non-Traditional Isotopes by SIMS and LA–MC–ICP–MS: Key Aspects and the Example of Mg Isotopes in Olivines and Silicate Glasses, *Reviews in Mineralogy and Geochemistry*, 2017, **82**, 127-163.

18. D. Trail, P. Boehnke, P. S. Savage, M.-C. Liu, M. L. Miller and I. Bindeman, Origin and significance of Si and O isotope heterogeneities in Phanerozoic, Archean, and Hadean zircon, *Proceedings of the National Academy of Sciences*, 2018, **115**, 10287.

19. J.-L. Guo, Z. Wang, W. Zhang, F. Moynier, D. Cui, Z. Hu and M. N. Ducea, Significant Zr isotope variations in single zircon grains recording magma evolution history, *Proceedings of the National Academy of Sciences*, 2020, **117**, 21125.

20. L. Liu, J. Mavrogenes, P. Holden and T. Ireland, Quadruple sulfur isotopic fractionation during pyrite desulfidation to pyrrhotite, *Geochimica et Cosmochimica Acta*, 2020, **273**, 354-366.

21. T. Iizuka and T. Hirata, Improvements of precision and accuracy in in situ Hf isotope microanalysis of zircon using the laser ablation-MC-ICPMS technique, *Chemical Geology*, 2005, **220**, 121-137.

22. C. Holmden and N. Bélanger, Ca isotope cycling in a forested ecosystem, *Geochimica et Cosmochimica Acta*, 2010, **74**, 995-1015.

23. M. Sharma, D. A. Papanastassiou, G. J. Wasserburg and R. F. Dymek, The issue of the terrestrial record of ^{146}Sm, *Geochimica et Cosmochimica Acta*, 1996, **60**, 2037-2047.

24. K. R. Ludwig, Optimization of multicollector isotope-ratio measurement of strontium and neodymium, *Chemical Geology*, 1997, **135**, 325-334.

25. R. Fukai, T. Yokoyama and S. Kagami, Evaluation of the long-term fluctuation in isotope ratios measured by TIMS with the static, dynamic, and multistatic methods: A case study for Nd isotope measurements, *Int. J. Mass Spectrom.*, 2017, **414**, 1-7.

26. G. Caro, B. Bourdon, J.-L. Birck and S. Moorbath, High-precision ^{142}Nd/^{144}Nd measurements in terrestrial rocks: Constraints on the early differentiation of the Earth's mantle, *Geochimica et Cosmochimica Acta*, 2006, **70**, 164-191.

27. R. Fiedler and D. Donohue, Pocket sensitivity calibration of multicollector mass spectrometers, *Fresenius Zeitschrift für Analytische Chemie*, 1988, **331**, 209-213.

28. C. Bayne, D. Donohue and R. Fiedler, Multidetector calibration for mass spectrometers, *International Journal of Mass Spectrometry and Ion Processes*, 1994, **134**, 169-182.

29. I. Wendt and G. Haase, Dynamic double collector measurement with cup efficiency factor determination, *Chemical Geology*, 1998, **146**, 99-110.

30. K. L. Ramakumar and R. Fiedler, Calibration procedures for a multicollector mass spectrometer for cup efficiency, detector amplifier linearity, and isotope fractionation to evaluate the accuracy in the total evaporation method, *Int. J. Mass Spectrom.*, 1999, **184**, 109-118.

31. M. F. Thirlwall, Long-term reproducibility of multicollector Sr and Nd isotope ratio analysis, *Chemical Geology: Isotope Geoscience section*, 1991, **94**, 85-104.

32. A. Makishima and E. Nakamura, Calibration of Faraday cup efficiency in a multicollector mass spectrometer, *Chemical Geology: Isotope Geoscience section*, 1991, **94**, 105-110.

33. M. F. Thirlwall and R. Anczkiewicz, Multidynamic isotope ratio analysis using MC–ICP–MS and the causes of secular drift in Hf, Nd and Pb isotope ratios, *Int. J. Mass Spectrom.*, 2004, **235**, 59-81.

34. Y. Fukami, M. Tobita, T. Yokoyama, T. Usui and R. Moriwaki, Precise isotope analysis of sub-nanogram lead by total evaporation thermal ionization mass spectrometry (TE-TIMS) coupled with a ^{204}Pb–^{207}Pb double spike method, *J. Anal. At. Spectrom.*, 2017, **32**, 848-857.

35. T. Miyazaki, B. S. Vaglarov and J.-I. Kimura, Determination of relative Faraday cup efficiency factor using exponential law mass fractionation model for multiple collector thermal ionization mass spectrometry, *Geochemical Journal*, 2016, **50**, 445-447.

36. A. S. G. Roth, B. Bourdon, S. J. Mojzsis, M. Touboul, P. Sprung, M. Guitreau and J. Blichert-Toft, Inherited ^{142}Nd anomalies in Eoarchean protoliths, *Earth Planet. Sci. Lett.*, 2013, **361**, 50-57.

37. T. Yokoyama, Y. Fukami, W. Okui, N. Ito and H. Yamazaki, Nucleosynthetic strontium isotope anomalies in carbonaceous chondrites, *Earth Planet. Sci. Lett.*, 2015, **416**, 46-55.

38. B. L. A. Charlier, C. Ginibre, D. Morgan, G. M. Nowell, D. G. Pearson, J. P. Davidson and C. J. Ottley, Methods for the microsampling and high-precision analysis of strontium and rubidium isotopes at single crystal scale for petrological and geochronological applications, *Chemical Geology*, 2006, **232**, 114-133.

39. N. E. Holden, T. B. Coplen, J. K. Böhlke, L. V. Tarbox, J. Benefield, d. L. J. R., P. G. Mahaffy, G. O'Connor, E. Roth, D. H. Tepper, T. Walczyk, M. E. Wieser and S. Yoneda, IUPAC Periodic Table of the Elements and Isotopes (IPTEI) for the Education Community (IUPAC Technical Report), *Pure and Applied Chemistry*, 2018, **90**, 1833-2092.

40. U. Hans, High-precision strontium isotope measurements on meteorites: Implications for the origin and timing of volatile depletion in the inner solar system, Ph.D. thesis, ETH Zurich, 2013.

41. A. K. Kaw, *Introduction to Matrix Algebra*, University of South Florida, 2002.

42. D. W. Davis, A simple method for rapid calibration of faraday and ion-counting detectors on movable multicollector mass spectrometers, *Journal of Mass Spectrometry*, 2020, **55**, e4511.

43. F. Albarède and B. Beard, Analytical methods for non-traditional isotopes, *Reviews in Mineralogy and Geochemistry*, 2004, **55**, 113-152.

44. J.-I. Kimura, Q. Chang, N. Kanazawa, S. Sasaki and B. S. Vaglarov, High-precision in situ analysis of Pb isotopes in glasses using 10^{13} Ω resistor high gain amplifiers with ultraviolet femtosecond laser ablation multiple Faraday collector inductively coupled plasma mass spectrometry, *J. Anal. At. Spectrom.*, 2016, **31**, 790-800.